Drug Delivery and Translational Research (2021) 11:1509–1519
https://doi.org/10.1007/s13346-021-01003-7

ORIGINAL ARTICLE

Mannose-conjugated chitosan nanoparticles for delivery of Rifampicin to Osteoarticular tuberculosis

Pratiksha Prabhu[1] · Trinette Fernandes[1] · Pramila Chaubey[2] · Parvinder Kaur[3] · Shridhar Narayanan[3] · Ramya VK[3] · Sujata P. Sawarkar[1]

Accepted: 12 May 2021 / Published online: 21 May 2021

Abstract

Tuberculosis (TB) is a potentially fatal contagious disease and is a second leading infectious cause of death in the world. Osteoarticular TB is treated using standard regimen of 1st and 2nd line anti-tubercular drugs (ATDs) for extensive period of 8–20 months. These drugs are commonly administered in high doses by oral route or by intravenous route, because of their compromised bioavailability. The common drawbacks associated with conventional therapy are poor patient compliance due to long treatment period, frequent and high dosing, and toxicity. This aspect marks for the need of formulations to eliminate these drawbacks. MTB is an intracellular pathogen of mononuclear phagocyte. This attribute makes nanotherapeutics an ideal approach for MTB treatment as macrophages capture nano forms. Polymeric nanoparticles are removed from the body by opsonization and phagocytosis, which forms an ideal strategy to target macrophage containing mycobacteria. To further improve targetability, the nanoparticles are conjugated with ligand, which serves as an easy substrate for the receptors present on the macrophage surface. The purpose of present work was to develop intra-articular injectable in situ gelling system containing polymeric nanoparticles, which would have promising advantages over conventional method of treatment. The rationale behind formulating nanoparticle incorporated in situ gel-based system was to ensure localization of the formulation in intra-articular cavity along with sustained release and conjugation of nanoparticles with mannose as ligand to improve uptake by macrophages. Rifampicin standard ATD was formulated into chitosan nanoparticles. Chitosan with 85% degree of deacetylation (DDA) and sodium tripolyphosphate (TPP) as the crosslinking agent was used for preparing nanoparticles. The percent entrapment was found to be about 71%. The prepared nanoparticles were conjugated with mannose. Conjugation of ligand was ascertained by performing Fourier transformed infrared spectroscopy. The particle size was found to be in the range of 130–140 nm and zeta potential of 38.5 mV. Additionally, we performed scanning electron microscopy to characterize the surface morphology of ligand-conjugated nanoparticles. The conjugated chitosan nanoparticles were incorporated into in situ gelling system comprising Poloxamer 407 and HPMC K4M. The gelling system was evaluated for viscosity, gelling characteristics, and syringeability. The drug release from conjugated nanoparticles incorporated in in situ gel was found to be about 70.3% at the end of 40 h in simulated synovial fluid following zero-order release kinetics. Based on the initial encouraging results obtained, the nanoparticles are being envisaged for ex vivo cellular uptake study using TB-infected macrophages

Keywords Osteoarticular tuberculosis · Chitosan · Mannose · Ligand · Conjugation

✉ Sujata P. Sawarkar
sujata.sawarkar@bncp.ac.in; sujatasawarkar19@gmail.com

Pratiksha Prabhu
pratu2395@gmail.com

Trinette Fernandes
trinette.fernz@gmail.com

Pramila Chaubey
cpramil@gmail.com

Parvinder Kaur
parvinder.kaur@fndr.in

Shridhar Narayanan
shridhar.narayanan@fndr.in

[1] Department of Pharmaceutics, SVKM's Dr Bhanuben Nanavati College of Pharmacy, University of Mumbai, Mumbai, India

[2] Department of Pharmaceutics, College of Pharmacy, Shaqra University, Al-Dawadmi, Saudi Arabia

[3] Foundation for Neglected Disease Research, Veerapura Village, Doddaballapur, Bangalore 561203, India

Abbreviations

TB	Tuberculosis
BJTB	Bone and joint tuberculosis
MTB	Mycobacterium
ATDs	Anti-tubercular drugs
TPP	Sodium tripolyphosphate
STAB	Sodium triacetoxy borohydride
HPMC	Hydroxy propyl methyl cellulose
DDA	Degree of deacetylation
%EE	Percent entrapment efficiency
FTIR	Fourier transformed infrared spectroscopy
DSC	Differential scanning calorimetry
MCNPs	Mannose-conjugated chitosan nanoparticles
PDI	Polydispersity index

Introduction

Tuberculosis (TB) is a potentially fatal contagious disease and is a second leading infectious cause of death in the world. Bone and joint TB (BJTB)/osteoarticular TB is a secondary form of TB occurring most commonly due to hematogenous seeding of mycobacterium (MTB) from the primary site of infection [1]. The prevalence of the disease is around 30 million globally, and approximately 30% or 10 million cases exist in India. Osteoarticular tuberculosis is found in about 10–20% of all diagnosed tuberculosis, which is the most common extrapulmonary tuberculosis. Osteoarticular disease is seen after the principal lesions of lungs spread phenomenally via lymph nodes [2]. Osteoarticular TB is treated using standard regimen of 1st and 2nd line anti-tubercular drugs (ATDs) for extensive period of 8–20 months. The predisposing factors affecting success of therapy include patient compliance, therapy regimen, malnutrition, pre-existing diseases [3, 4]. Osteoarticular TB behaves differently from pulmonary TB. The treatment is comparatively complex than pulmonary TB and requires combination therapy for longer duration around a year or two as destroying dormant population is quite challenging. Inadequate killing of MTB can cause relapse with variation in treatment response [5, 6] The conventional therapy regimens have been successful to some extent in bringing about, if not complete but at least partial eradication of TB. The drawbacks associated with currently available treatment mainly include long period of treatment, toxicity, and increased frequency of dosing [7]. All these factors lead to discontinuation of the therapy even before the completion of treatment. The repercussions of discontinued therapy are increased probability of MTB bacteria developing resistance to drug leading to ineffectiveness of treatment [8]. Most of the drugs used for the treatment of TB belong to BCS II or IV. It is because of their compromised solubility or permeability resulting into poor bioavailability. As a result, they are required to be administered in high doses by the oral route or by intramuscular/intravenous route [9]. This marks for the need of evolving and developing modified formulations to eliminate these drawbacks. Nanocarriers have the potential to address some of the challenges like an ideal approach for MTB treatment as macrophages capture nanoforms with or without surface modifications [10]. Various nanocarrier systems that have been extensively studied are polymeric and lipid nanoparticles, polymeric micelle, and carbon nanotubes [11]. The peculiar characteristic of nanocarriers is that they are removed from the body by opsonization and phagocytosis. This attribute forms an effective strategy to target macrophage containing mycobacteria. Although nano formulations can play an important role in effective treatment of TB, their role in enhancing targetability is sometimes limited. In order to improve the targetability of nanoformulations, various ligands specific to the mycobacteria cell components or macrophage receptor are being envisaged [12]. Ligand-anchored therapy is a strong and effective approach to execute drug delivery into selective target cells. Studies have shown that apart from targeting, ligands provide shielding effect to drug carrier and prolong its circulation time in the bloodstream [13]. In the present work, we have formulated chitosan nanoparticles loaded with first-line therapy drug Rifampicin. The polymeric nanoparticles were conjugated with mannose as targeting ligand. The conjugated drug-loaded polymeric nanoparticles were incorporated into intra-articular injectable in situ gelling system. The rationale behind developing this formulation strategy was to ensure localization of the formulation in intra-articular cavity along with sustained release and conjugation of nanoparticles with mannose as ligand to improve uptake by macrophages. It has been observed that mannose receptors are over expressed during mycobacterial infection. Hence, mannosylated nanoparticle can serve as effective cargo to deliver the drug in to macrophageal cells hosting the mycobacteria [14–17]

Materials and method

The active pharmaceutical ingredient, Rifampicin, was obtained as a gift sample from Lupin Pharmaceuticals Ltd., India. The natural polymer, chitosan with 85% degree of acetylation from MatsyaFed, India, and other excipients such as hydroxy propyl methyl cellulose K4M from Colorcon India Pvt. Ltd.), Poloxamer 407 (Sigma-Aldrich), mannose (Lobachemie Ltd.), sodium tripolyphosphate (TPP) (Lobachemie Ltd.), and sodium triacetoxy borohydride (STAB) (Lobachemie Ltd.) were obtained as gift sample. The other chemicals and solvents required for experimentation were procured from SD Fine Chemicals Ltd.

Preparation of Rifampicin-loaded mannose-conjugated chitosan nanoparticles

In order to formulate Rifampicin-loaded mannose-conjugated chitosan nanoparticles, mannose-conjugated chitosan polymer was prepared. Mannose conjugation was obtained by performing reductive deamination of chitosan with D-mannose [18]. Chitosan was dissolved in lactic acid solution (1% *w*/*v*) using overhead stirrer. This was followed by addition of aqueous solution of STAB and D-mannose to the chitosan solution. The polymer was allowed to react with STAB and D-mannose for a period of 2 days. On completion of reaction, unreacted mannose and STAB were removed by dialysis method. For purification process, the conjugated polymer was dialyzed using a dialysis membrane with molecular weight cutoff of 12–14 kDa (Himedia 150) in double distilled water. The process was continued for 72 h. The prepared polymer was dried using spray drier (Labultima LU 222) maintaining inlet temperature at 50 °C [19]. The process was optimized for parameters like % STAB concentration and % D-mannose concentration. The formation of conjugated polymer was ascertained by Fourier transformed infrared spectroscopy. Rifampicin, the model drug used for loading nanoparticles, was subjected to preformulation studies wherein the purity of drug was assessed by performing differential scanning calorimetry (DSC) and FTIR (Shimadzu IRAffinity-IS) (Fig. 1). Chitosan nanoparticles were produced by ionic gelation method using TPP as crosslinking agent [20]. In order to prepare nanoparticles, the conjugated polymer was dissolved in 2% *w*/*v* lactic acid solution under magnetic stirring for 2 h [21]. On complete dissolution of polymer, the pH of the solution was adjusted to 5 using 1 M sodium hydroxide. Rifampicin was first dissolved in dimethylsulfoxide and Tween 80 mixture and then added to TPP solution. The process was optimized for parameters like DDA of chitosan polymer concentration, TPP concentration, and drug and Tween 80 concentration, stirring speed. For the sake of comparative evaluation, Rifampicin was encapsulated in non-conjugated chitosan nanoparticles.

Evaluation of Rifampicin-loaded mannose-conjugated chitosan nanoparticles

Rifampicin-loaded mannose-conjugated chitosan nanoparticles (MCNPs) were evaluated for physicochemical characteristics like entrapment efficiency, particle size distribution, and measurement of polydispersity index using laser diffraction measurement (Malvern Zetasizer Nano ZS), zeta potential (mV), and surface morphology by scanning

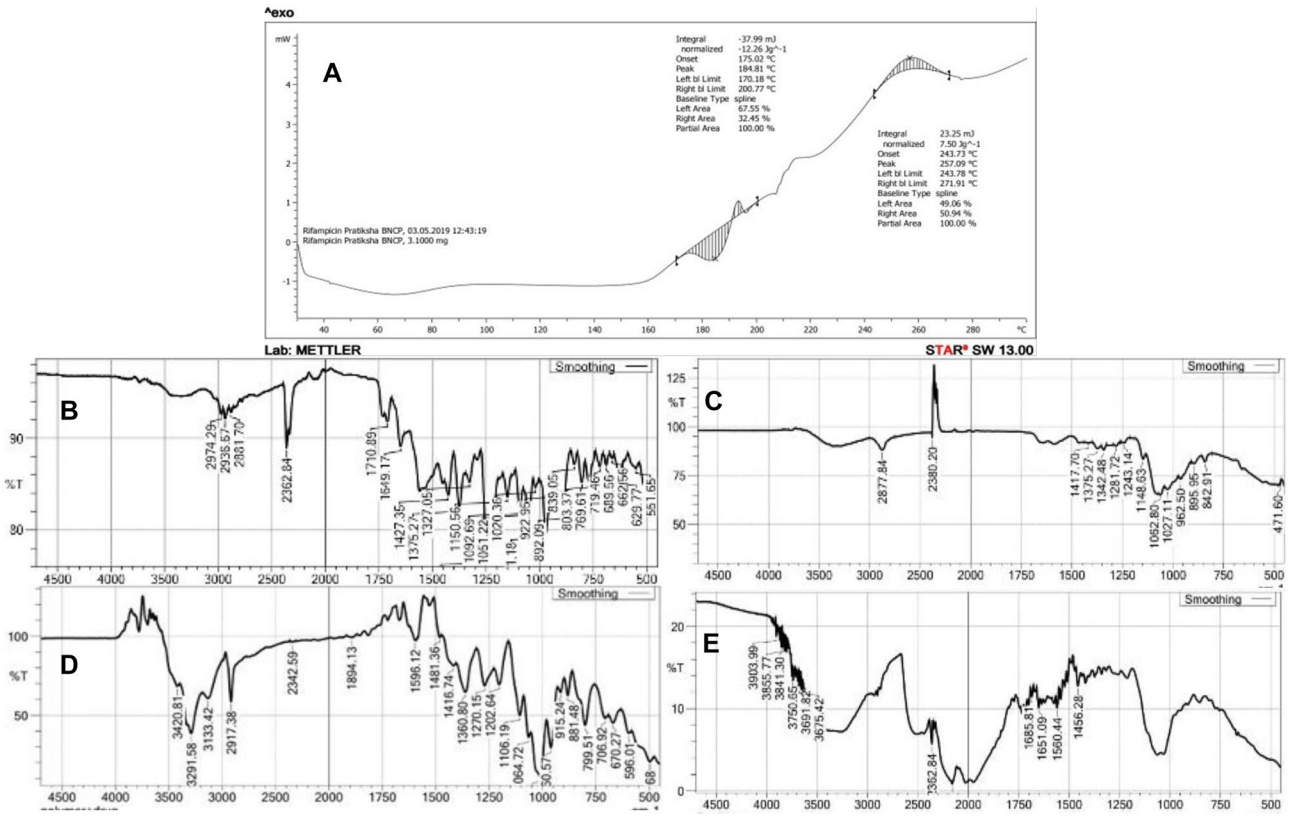

Fig. 1 **A** DSC endotherm of Rifampicin, **B** FTIR spectra of Rifampicin, **C** FTIR spectra of chitosan, **D** FTIR spectra of mannose, and **E** FTIR spectra of chitosan-mannose conjugate polymer

electron microscopy (Zeiss Evo 50) [22]. Drug release studies were performed by diffusion in simulated synovial fluid (pH 7.4) [23] and simulated endosomal fluid (pH 5.2) [24] using dialysis membrane (Himedia 150). The drug release kinetics was predicted by computing regression coefficient of zero order, first order, Higuchi, and Korsmeyer-Peppas models [25].

Development and evaluation of in situ gelling system containing mannose-conjugated chitosan nanoparticles

Various gelling agents such as chitosan, deacetylated gellan gum, sodium alginate, and Poloxamer 407 in combination with HPMC K4M were used to formulate in situ gelling system [26]. The composition and proportion of the polymers were optimized based on clarity, syringeability, gelation time, and gelling capacity. Rifampicin-loaded mannose-conjugated chitosan nanoparticles were incorporated in in situ gelling system and evaluated for drug release for period of 40 h [27].

Determination of in vitro activity of Rifampicin in mannose-conjugated chitosan nanoparticles against *Mycobacterium tuberculosis*

Minimum inhibitory concentration (MIC) of Rifampicin formulated as plain and mannose-conjugated chitosan nanoparticles was tested against *Mycobacterium tuberculosis* (*Mtb*) H37Rv ATCC 27,294 wild-type strain. Minimum inhibitory concentration (MIC) was determined by the standard broth dilution method [28–30]. Briefly, the test compounds were dissolved in acetate buffer pH 5.2, serially double-diluted in a 10-concentration dose response (10-DR) ranging from 32 to 0.0625 µg/mL in 96-well plates in Middlebrook 7H9 media. The *Mtb* culture was added as 200 µL ($3–7 \times 10^5$ cfu/mL) to the respective assay plates in each well to all columns, except the media control (200 µL of media). QC included media controls, growth controls, and reference drug inhibitors (Rifampicin and Isoniazid). The assay plates were incubated at 37 °C/6 days. Resazurin dye was added to all the wells including the media and culture controls and the plates were incubated at 37 °C/1 day. The results were noted on the 7th day as "blue to pink" colorimetric readout. The blue wells indicated inhibition of growth, while the pink wells indicated uninhibited growth. The MIC was the minimum concentration of the formulations that completely inhibited the growth of bacteria. The results are mentioned in Table 4.

Results and discussion

Preparation of Rifampicin-loaded mannose-conjugated chitosan nanoparticles

Rifampicin is a bactericidal drug which interferes with the synthesis of nucleic acids by inhibiting DNA-dependent RNA-polymerase. Rifampicin binds to the pocket of RNA polymerase beta subunit within the DNA/RNA channel but away from the active site. The drug is active against Gram-positive bacteria, mycobacterium species, and some Gram-negative bacteria [31]. The drug shows good pH-dependent solubility at lysosomal pH of the macrophage. By conventional route, Rifampicin is required to be administered in high and frequent doses in order to exhibit therapeutic effect. In order to counter and nullify some of these drawbacks, we have formulated intra-articular injectable in situ gelling system containing polymeric nanoparticles. The objective behind formulating nanoparticle incorporated in situ gel-based system is to ensure localization of the formulation in intra-articular cavity along with sustained release and easy access of nanoparticles to bone and joints, thus minimizing bio-distribution to other parts. The drug was evaluated for preformulation testing to ascertain its purity and compliance with compendial standards. An endothermic peak assignable to melting point of Rifampicin was observed at 183–185 °C indicating purity of active pharmaceutical ingredient (Fig. 1A). FTIR peaks were observed at wave numbers peculiar to the functional groups present in molecular structure of Rifampicin that further confirmed the suitability and quality of the active pharmaceutical ingredient (Fig. 1B).

In the pre-optimization experiments, chitosan nanoparticles were prepared during polymer of different DDA. The objective of performing these experimental trials was to select the suitable grade of chitosan, for preparing conjugated polymer. Polymeric nanoparticles were prepared using chitosan 75% and chitosan 85%, respectively, along with TPP 1% as crosslinker (supplementary section). Nanoparticles prepared using 75% and 85% DDA were subjected to microscopic observation using Motic. Chitosan with 75% DDA yielded thread like aggregates and instant gelation of particles was observed. Nanoparticles obtained from chitosan with 85% DDA were found to be spherical (Fig. 2).

The optimum proportion of chitosan and mannose was obtained by assessing the quality of conjugated polymer prepared using varying concentrations of chitosan and mannose and STAB as reducing agent (Table 1). Mannose-conjugated chitosan polymer prepared by spray drying when freshly prepared was found to be off white and free flowing powder. However, as the time elapsed, a drastic

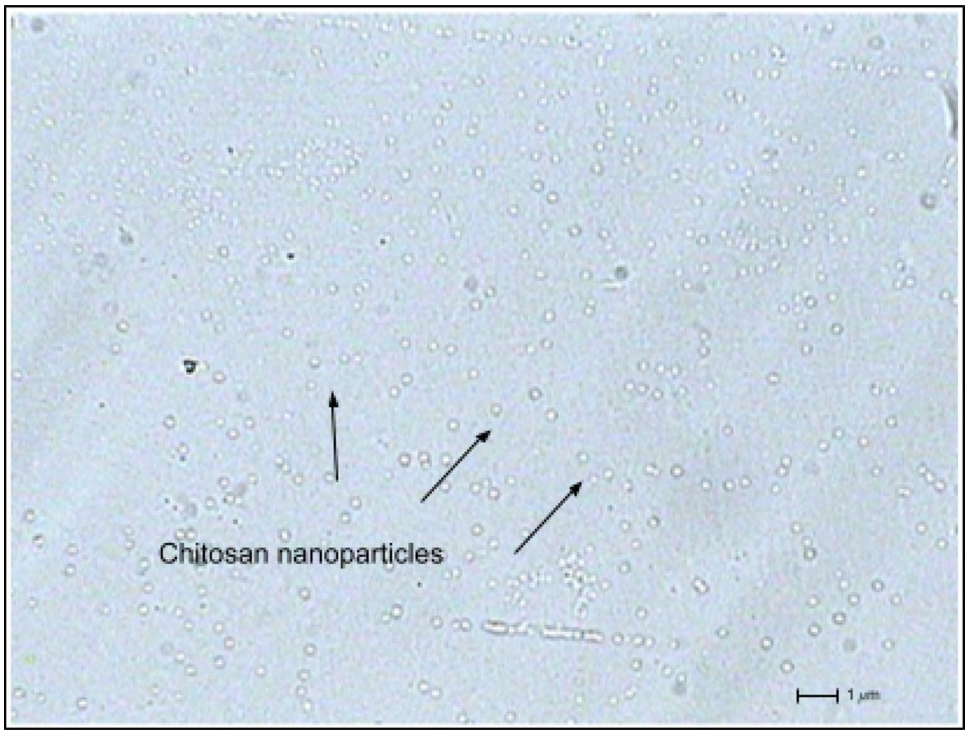

Fig. 2 Spherical particles with chitosan 85% DDA in size range of 0.5–0.9 µm

change in color from off white to brown was observed for conjugated polymer. The time required for this color change was found to be dependent on mannose and STAB proportion. Batch CM5 with reduced concentration of STAB and chitosan and mannose in the ratio 3:1 gave stable free flowing powder. The conjugation of mannose with chitosan was ascertained by overlaying the FTIR spectra of chitosan and mannose with that of conjugated polymer (supplementary data for Table and Fig. 1C-E). In the FTIR spectra of chitosan–mannose conjugate, 2 peculiar peaks were observed at 1560.44 cm^{-1} and 1456.28 cm^{-1} indicating N-H bending of secondary amine and C=N stretch, respectively. The formation of Schiff's base (R-CH=N-R bond) by ring opening reaction of mannose followed by reaction of the aldehyde group with amino group of chitosan as proved by the above mentioned peaks confirmed the formation of mannose-conjugated chitosan (Fig. 1E)

Table 1 Optimization of mannose-conjugated chitosan polymer

Batch No	Chitosan (g)	D-mannose (g)	STAB (g)
CM1	0.6	0.2	0.2
CM2	0.8	0.3	0.3
CM3	0.8	0.2	0.2
CM4	2	1	0.5
CM5	3	1	0.15

In further experimental study, polymeric nanoparticles were prepared using varying concentrations of mannose-conjugated chitosan, TPP, and Tween 80. The speed was maintained in the range of 4000–6000 rpm (Table 2). Drug entrapment efficiency of nanoparticle batches M1 and M2 prepared using chitosan 0.5% and TPP 0.25% with ethanol as solvent was found to be less than 40%. Batches M3–M5 prepared without Tween 80 were found to be unstable and formed turbid dispersion on storage. Batch M8 with chitosan 1%, TPP 0.75%, and Tween 80% 1% yielded stable nanodispersion and drug entrapment efficiency of about 70.86%. Batch M8 was subjected to further detailed characterization.

Evaluation of Rifampicin-loaded mannose-conjugated chitosan nanoparticles

Rifampicin-loaded mannose-conjugated chitosan nanoparticles of batch M8 were assessed for physicochemical characteristics. For comparative evaluation, nanoparticles were prepared using plain chitosan. In order to determine entrapment efficiency, 10 mL of the dispersion was centrifuged at 15,000 rpm at 4 °C for 20 min. The supernatant was collected, diluted with methanol, and analyzed for free drug. Entrapment efficiency was determined by using the following formula: [32]

$$\%\text{Entrapment efficiency} = \frac{\text{Total drug} - \text{Free drug} \times 100}{\text{Total drug}}$$

Table 2 Optimization batches, observation of percent entrapment efficiency (% EE) of rifampicin-loaded D-mannose-conjugated chitosan nanoparticles (MCNPs)/Rifampicin-loaded chitosan nanoparticles (CNPs)

Batch No	Chitosan (%)	TPP (%)	Drug (mg)	Tween 80 (%)	Solvent	Speed (RPM)	%EE (MCNPs)	%EE (CNPs)	Observations
M1	0.5	0.25	50	-	Ethanol	4000	32.99	-	Few particles observed under motic
M2	0.5	0.25	50	0.4	Ethanol	4500	39.94	-	
M3	0.5	0.25	100	-	DMSO	4500	39.67	-	Turbid dispersion formed after 2 days
M4	0.5	0.75	100	-	DMSO	4500	42.63	-	
M5	1	0.25	100	-	DMSO	4500	40.25	-	
M6	1	0.5	100	0.4	DMSO	4500	52	52.69	Stable nanodispersion obtained
M7	1	0.5	150	1	DMSO	4500	65.64	66.23	
M8	1	0.75	150	1	DMSO	6000	70.86	73.86	

% Entrapment efficiency of mannose-conjugated chitosan nanoparticles and chitosan nanoparticles was found to be 70.86 and 73.86, respectively, indicating appreciable drug loading capacity of formulation and conjugation of mannose with chitosan did not have significant effect on entrapment efficiency.

Particle size determined by dynamic light scattering indicated size of 138 nm with PDI of 0.173 for plain chitosan nanoparticles whereas for mannose-conjugated chitosan nanoparticles, the size was observed to be 142 nm with PDI of 0.154 (Fig. 3A and B). It was concluded that the coupling of mannose in chitosan caused slight

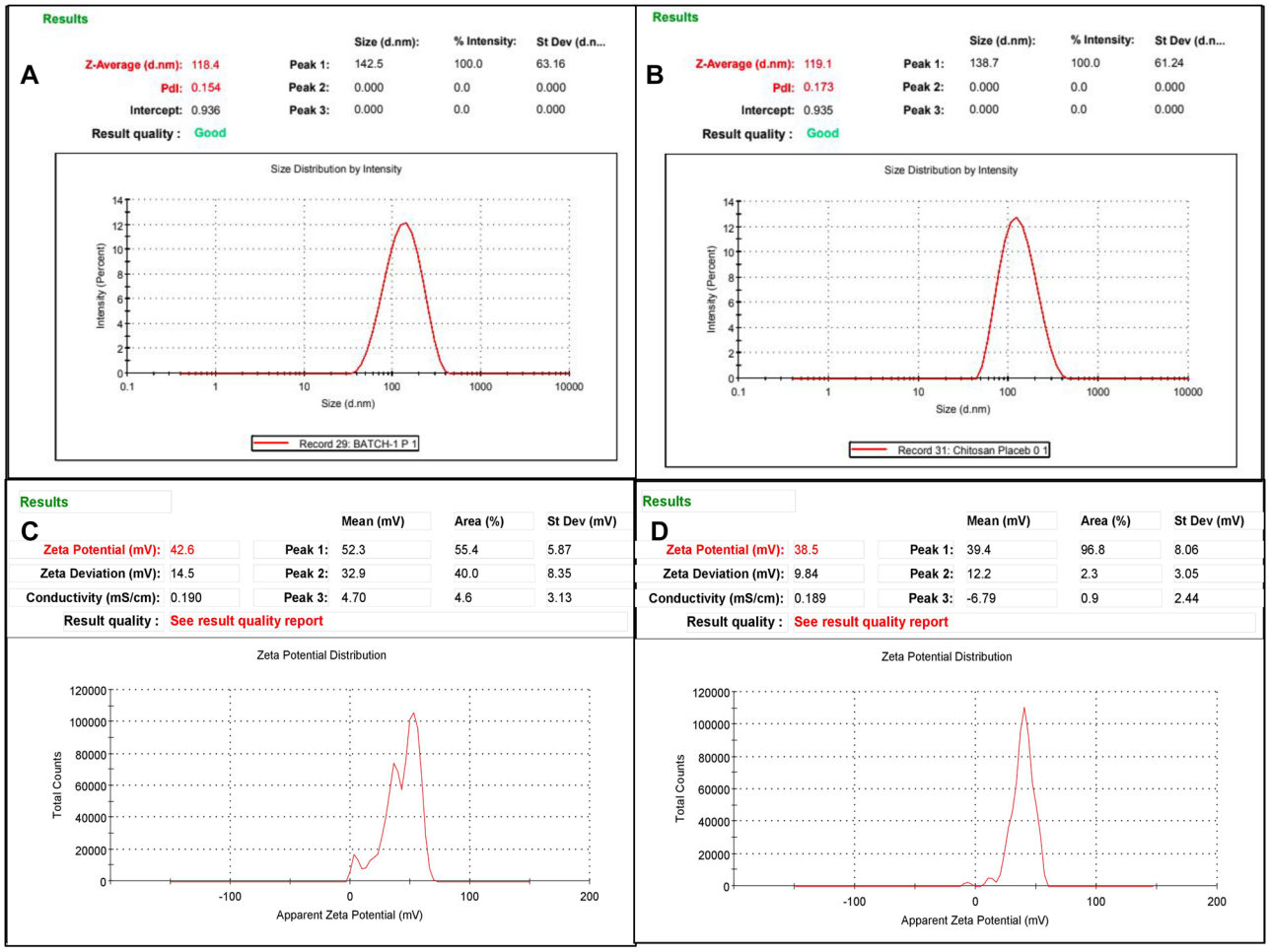

Fig. 3 **A** Particle size of chitosan nanoparticles, **B** particle size of mannose-conjugated chitosan nanoparticles, **C** zeta potential of non-conjugated chitosan nanoparticles, and **D** zeta potential of mannose-conjugated chitosan nanoparticles

increase in the size of nanoparticles prepared using conjugated polymer. Zeta potential of chitosan particles was found to be 42.6 mV whereas zeta potential of mannose-conjugated chitosan particles was found to be 38.5 mV. The reduction in zeta potential and sharper peak was attributed to conjugation of mannose to chitosan resulting in reduction of primary amino groups as they couple to CHO groups of mannose (Fig. 3C and D) [33].

Surface morphology of mannose-conjugated chitosan nanoparticles and chitosan nanoparticles was compared by performing scanning electron microscopy (SEM) (Fig. 4). The formulations were placed on circular aluminum stubs using double adhesive tape, coated with gold in HUS-5 GB vacuum evaporator, and observed in SEM at an acceleration voltage of 10 kV and a magnification of 5000× [34]. SEM images revealed that plain chitosan nanoparticles were spherical whereas mannose-conjugated chitosan nanoparticles were found to be platelet shaped with pitted surface. This peculiar characteristic was attributed because of conjugation of mannose with chitosan and we are postulating that this peculiar shape will enhance the uptake of nanoparticles by macrophages.

Dialysis sac method was used to determine their lease of drug from nanoparticulate formulation. Drug release studies from mannose-conjugated chitosan nanoparticles were performed in simulated synovial fluid pH 7.4 and simulated endosomal fluid pH 5.2 (Fig. 5 and supplementary section). The drug release was found to be about 70.7% at the end of 12 h in simulated synovial fluid whereas the drug release in simulated endosomal fluid was 89.17%. Higher percent drug release in simulated endosomal fluid was indicative of preferential uptake of nanoparticles by macrophages and drug release in its endosomal contents.

In order to understand the kinetics and mechanism of drug release, the results of in vitro drug dissolution studies of optimized formulation were fitted in various kinetics models like zero order (percent cumulative drug release vs. time), first order (log percent drug remaining vs. time), Higuchi's model (percent cumulative drug release vs. square root of time), and Korsmeyer-Peppas plot (log of percent cumulative drug released vs. log of time) (supplementary section). The regression coefficient values were computed and found to be 0.971, 0.903, 0.812, and 0.745 for zero order, first order, Higuchi and Korsmeyer-Peppas model, respectively. The higher value of regression for percent cumulative drug release vs. time indicated that drug release from conjugated chitosan nanoparticles followed zero-order kinetics.

Development and evaluation of in situ gelling system containing mannose-conjugated chitosan nanoparticles

Various gelling agents such as chitosan 75% DDA (1–2%), deacetylated gellan gum, sodium alginate (1–2%), Poloxamer 407 (10–15%) in combination with HPMC K4M (0.5%) were used to formulate in situ gelling system. The composition and proportion of the polymers were optimized based on clarity, syringeability, gelation time, and gelling capacity. Gellan gum being anionic polymer showed incompatibility with cationic chitosan nanoparticles; hence, it was not considered for further optimization. Poloxamer 407 (15%) in combination with HPMC formed a stable in situ gel at 37 °C when subjected to simulated synovial fluid (26, 35, 36) (Table 3). Rifampicin-loaded mannose-conjugated chitosan nanoparticles were incorporated in in situ gelling system and evaluated for

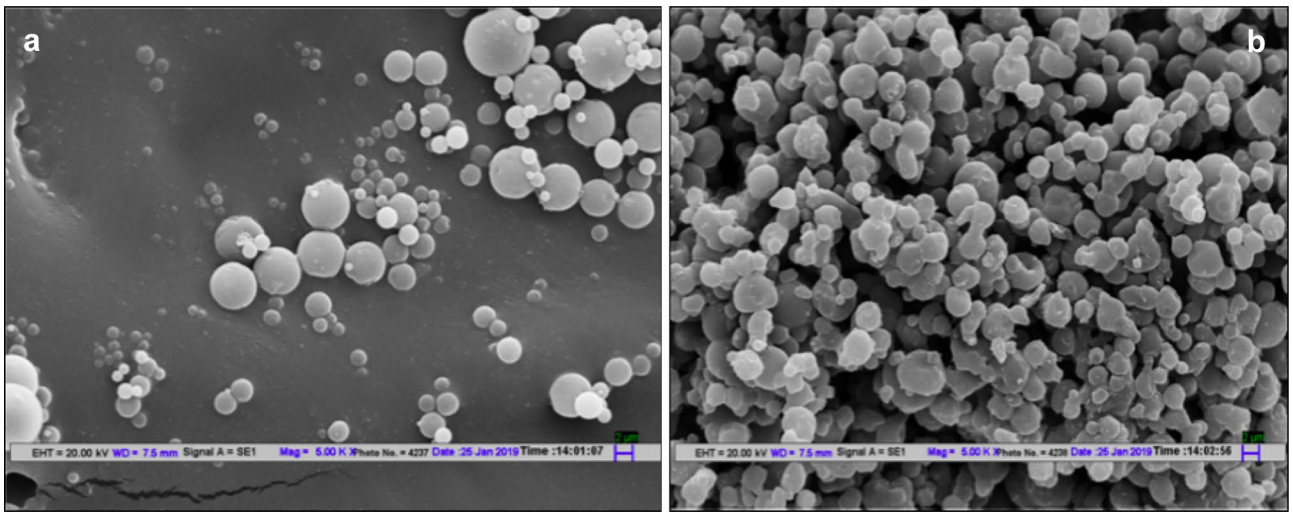

Fig. 4 **A** SEM image of chitosan nanoparticles and **B** SEM image of mannose-conjugated chitosan nanoparticles

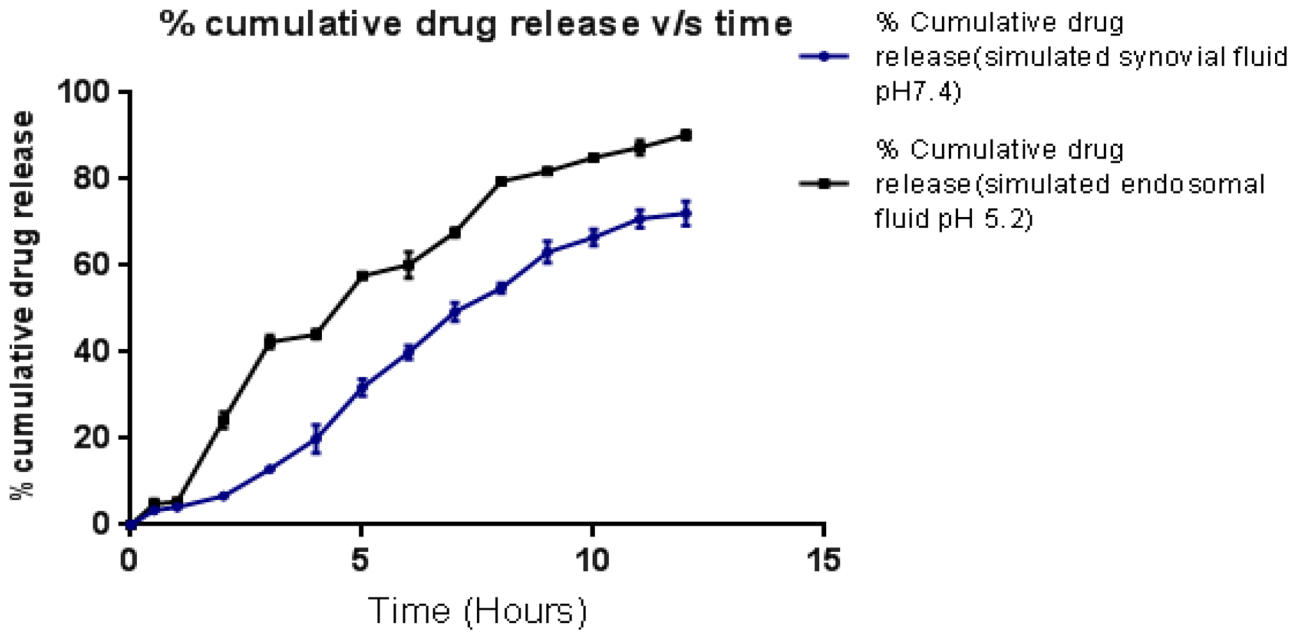

Fig. 5 Graph depicting percent cumulative drug release versus time for mannose-conjugated chitosan nanoparticles in simulated synovial fluid and simulated endosomal fluid

drug release in simulated synovial fluid for period of 40 h. Incorporation of nanoparticles in gelling system prolonged the drug release considerably. Cumulative percent release at the end of 40 h was about 70.3% (Fig. 6 and supplementary section).

The drug release kinetics was computed for nanoparticles incorporated in in situ gel (supplementary section). The higher value of regression coefficient for percent cumulative drug release vs. time ($R^2 = 0.836$) indicated that drug release from conjugated chitosan nanoparticles incorporated in in situ gel followed by zero-order kinetics.

Minimum inhibitory concentration of Rifampicin in mannose-conjugated CHITOSAN nanoparticles against *Mycobacterium tuberculosis*

Rifampicin formulated as chitosan nanoparticles with and without conjugation with mannose demonstrated minimal inhibitory concentration (MIC) of 0.009 µg/mL against *M. tuberculosis* H37Rv ATCC 27294 wild-type strain (Table 4).

Based on the microbiology results of the formulations, it is evident that Rifampicin is released efficiently from the formulation to provide concentrations sufficient to kill the *M.tb*. Also, conjugation of Rifampicin nanoparticles with mannose did not have any significant effect on inhibitory activity against *M.tb.*

Table 3 Evaluation of various polymers for the formation of in situ gel

Polymers	Gelling ability	Syringeability	Clarity	Inference
Gellan gum	Good	Good	Good	Incompatible with the polymeric nanoparticles
Chitosan	Poor	Good	Good	Gelling ability was not optimum
Sodium Alginate	Poor	Good	Good	Gelling ability was not optimum
Poloxamer 407 + HPMC	Good	Good	Good	Optimum gelling with good gelling ability of more than 12 h and good syringeability was observed

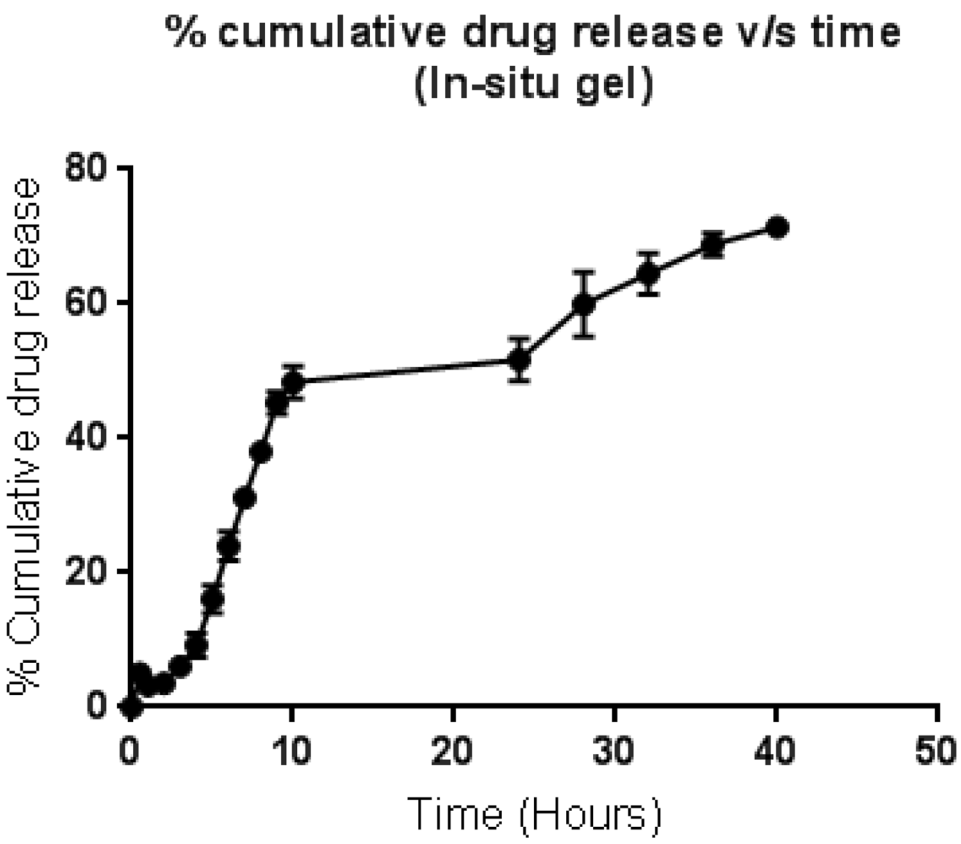

Fig. 6 Graph depicting percent cumulative drug release versus time for in situ gel loaded with mannose-conjugated chitosan nanoparticles in simulated synovial fluid

Table 4 MIC of Rifampicin-loaded nanoparticles (conjugated and non-conjugated) against *M. tuberculosis* H37Rv ATCC 27,294

Sr. No	Formulation tested against Mtb	MIC (μg/mL)
1	Rifampicin-loaded mannosylated chitosan nanoparticles (batch 1)	0.009
2	Rifampicin-loaded plain chitosan nanoparticles (batch 2)	0.009
3	Rifampicin (API used for formulation)	0.015
4	Placebo	> 32
QC	Rifampicin	0.0078
	Isoniazid	0.06

Conclusion

A promising targeted delivery system consisting of ligand-conjugated Rifampicin nanoparticles incorporated in in situ gel was developed to tackle the drawbacks associated with the conventional treatment of osteoarticular tuberculosis. Rifampicin-loaded mannose-conjugated chitosan nanoparticles were prepared by ionic gelation technique. Mannose-conjugated chitosan nanoparticles showed preferential drug release in endosomal fluid indicative of preferential uptake of nanoparticles by macrophages and drug release in its endosomal contents. In vitro drug release of mannose-conjugated Rifampicin nanoparticles incorporated in in situ gel system showed prolonged release for 40 h. Minimum inhibitory concentration of nanoparticles was found to be 0.009 μg/mL indicating that nanoparticles released sufficient concentration of active moiety to inhibit *Mycobacterium tuberculosis*. Based on the initial encouraging results obtained, the nanoparticles are being envisaged for ex vivo cellular uptake study using TB-infected macrophages.

Supplementary information The online version contains supplementary material available at https://doi.org/10.1007/s13346-021-01003-7.

Acknowledgements The authors wish to thank Sophisticated Analytical Instrument Facility, IIT-Bombay, Powai for their providing SEM analysis samples which are used in this manuscript.

Author contribution All authors contributed to the study and manuscript conception and design. Material preparation, data collection, and analysis and experiments were performed by Ms Pratiksha Prabhu and Ms. Trinette Fernandes. The research activity planning, execution, and supervision were carried out under the guidance of Dr Sujata Sawarkar and Dr Pramila Chaubey. Dr. Shridhar Dr Ramya VK and Dr. Parminder Kaur conducted the MIC studies of formulation against *M. tb.* All authors commented on previous versions of the manuscript, read, and approved the final manuscript.

Availability of data and materials The datasets generated during and/or analyzed during the current study are available from the corresponding author on reasonable request.

Declarations

Competing interests The authors declare no competing interests.

References

1. Bhowmik CD, Chandira RM, Jayakar B, Kumar KPS. Recent trends of drug used treatment of tuberculosis. J Chem Pharm Res. 2009;1(1):113–33.
2. Davidson PT, Horowitz I. Skeletal tuberculosis. A review with patient presentations and discussion. Am J Med. 1970;48(1):77–84.
3. Sequeira W, Co H, Block J. Osteoarticular tuberculosis: current diagnosis and treatment - PubMed. Am J Ther. 2000;7(6):393–8.
4. Procopie I, Popescu EL, Huplea V, Pleșea RM, Ghelase ȘM, Stoica GA, et al. Osteoarticular tuberculosis-brief review of clinical morphological and therapeutic profiles. Curr Heal Sci J. 2017;43(3):171–90.
5. Tuli SM, Brighton CT, Morton HE, Clark LW. The experimental induction of localised skeletal tuberculous lesions and their accessibility to streptomycin. J Bone Jt Surg - Ser B. 1974;56(3):551–9.
6. Pandita A, Madhuripan N, Pandita S, Hurtado RM. Challenges and controversies in the treatment of spinal tuberculosis. J Clin Tuber Other Mycobact Dis. 2020;1(19):100151.
7. Diseases C. WHO Report 2003 Global Tuberculosis Control. 2003; Accessed 30 March 2021
8. Sawarkar SP. Targeting approaches for effective therapeutics of bone tuberculosis abstract symptoms of bone tuberculosis. J Pharm Microbiol. 2017;3(1):1–3.
9. Chan ED, Iseman MD. Clinical review Current medical treatment for tuberculosis. Br Med J. 2002;325(7375):1282–6.
10. Organization WH. Anti-tuberculosis drug resistance in the world Third Global Report The WHO/IUATLD Global Project on Anti-tuberculosis Drug Resistance Surveillance [Internet]. 1999 [cited 2021 Mar 30].
11. Sosnik A, Glisoni R, Moretton MA, Carcaboso ÁM, Glisoni RJ, Chiappetta DA. New old challenges in tuberculosis: potentially effective nanotechnologies in drug delivery. Adv Drug Deliv Rev. 2009;62:547–59.
12. Lee J, Hartman M, Kornfeld H. Macrophage apoptosis in tuberculosis. Yonsei Med J. 2009;50(1):1–11.
13. Ramón-García S, Mikut R, Ng C, Ruden S, Volkmer R, Reischl M, et al. Targeting Mycobacterium tuberculosis and other microbial pathogens using improved synthetic antibacterial peptides. Am Soc Microbiol. 2013;57(5):2295–303.
14. Stahl PD. The mannose receptor and other macrophage lectins. Curr Biol. 1992;2(4):183.
15. Rajaram MVS, Brooks MN, Morris JD, Torrelles JB, Azad AK, Schlesinger LS. Mycobacterium tuberculosis activates human macrophage peroxisome proliferator-activated receptor γ linking mannose receptor recognition to regulation of immune responses. J Immunol. 2010;185(2):929–42.
16. Rajaram MVS, Arnett E, Azad AK, Guirado E, Ni B, Gerberick AD, et al. M. tuberculosis-initiated human mannose receptor signaling regulates macrophage recognition and vesicle trafficking by FcRγ-chain, Grb2, and SHP-1. Cell Rep. 2017;21(1):126–40.
17. Pawde DM, Viswanadh MK, Mehata AK, Sonkar R, Narendra, Poddar S, et al. Mannose receptor targeted bioadhesive chitosan nanoparticles of clofazimine for effective therapy of tuberculosis. Saudi Pharm J. 2020;28(12):1616–25.
18. Chaubey P, Mishra B. Mannose-conjugated chitosan nanoparticles loaded with rifampicin for the treatment of visceral leishmaniasis. Carbohydr Polym. 2014;101(1):1101–8.
19. Chaubey P, Patel RR, Mishra B. Development and optimization of curcumin-loaded mannosylated chitosan nanoparticles using response surface methodology in the treatment of visceral leishmaniasis. Expert Opin Drug Deliv. 2014;11(8):1163–81.
20. Abdelgawad AM, Hudson SM. Chitosan nanoparticles: polyphosphates cross-linking and protein delivery properties. Int J Biol Macromol. 2019;136:133–42.
21. Goñi MG, Tomadoni B, Roura SI, del Rosario Moreira M. Lactic acid as potential substitute of acetic acid for dissolution of chitosan: preharvest application to butterhead lettuce. J Food Sci Technol. 2017;54(3):620–6.
22. Vandervoort J, Ludwig A. Preparation and evaluation of drug-loaded gelatin nanoparticles for topical ophthalmic use. Eur J Pharm Biopharm. 2004;57(2):251–61.
23. Marques MRC, Loebenberg R, Almukainzi M. Simulated biological fluids with possible application in dissolution testing. Dissolution Technol. 2011;18(3):15–28.
24. Rabel M, Warncke P, Grüttner C, Bergemann C, Kurland HD, Müller R, et al. Simulation of the long-term fate of superparamagnetic iron oxide-based nanoparticles using simulated biological fluids. Nanomedicine. 2019;14(13):1681–706.
25. Thing M, Mertz N, Ågårdh L, Larsen SW, Østergaard JLC. Simulated synovial fluids for in vitro drug and prodrug release testing of depot injectables intended for joint injection. J Drug Deliv Sci Technol. 2019;49(1):169–76.
26. Talasaz AHH, Ghahremankhani AA, Moghadam SH, Malekshahi MR, Atyabi F, Dinarvand R. In situ gel forming systems of poloxamer 407 and hydroxypropyl cellulose or hydroxypropyl methyl cellulose mixtures for controlled delivery of vancomycin. J Appl Polym Sci. 2008;109(4):2369–74.
27. Levy G, Amherst NY. Kinetics of drug action: an overview. J Allergy Clin Immunol. 1985;78(4(2)):754–61.
28. Franzblau SG, Witzig RS, Mclaughlin JC, Torres P, Madico G, Hernandez A, et al. Rapid, low-technology MIC determination with clinical Mycobacterium tuberculosis isolates by using the microplate Alamar Blue Assay. J Clin Microbiol. 1998;36
29. Gail L. Woods, Barbara A. Brown-Elliott, Patricia S. Conville, Edward P. Desmond, Geraldine S. Hall, Grace Lin, et al. Susceptibility testing of Mycobacteria, Nocardia, and other aerobic actinomycetes - PubMed. 2nd ed. Wayne (PA): Clinical and Laboratory Standards Institute, editor. CLSI Standards: Guidelines for Health Care Excellence. 2011.
30. Kaur P, Ghosh A, Krishnamurthy RV, Bhattacharjee DG, Achar V, Datta S, et al. A High-Throughput Cidality Screen for Mycobacterium Tuberculosis. Manganelli R, editor. PLoS One. 2015;10(2):e0117577.
31. Drapeau CMJ, Grilli E, Petrosillo N. Rifampicin combined regimens for Gram-negative infections: data from the literature. Int J Antimicrob Agents. 2010;35(1):39–44.
32. Kumar PV, Asthana A, Dutta T, Jain NK. Intracellular macrophage uptake of rifampicin loaded mannosylated dendrimers. J Drug Target. 2006;14(8):546–56.
33. Patel BK, Parikh RH, Aboti PS. Development of oral sustained release Rifampicin loaded chitosan nanoparticles by design of experiment. J Drug Deliv. 2013;2013:1–10.
34. Lazaridou M, Christodoulou E, Nerantzaki M, Kostoglou M, Lambropoulou DA, Katsarou A, et al. Formulation and in-vitro characterization of chitosan-nanoparticles loaded with the iron chelator deferoxamine mesylate (DFO). Pharmaceutics. 2020;12(3).

35. Mayol L, Quaglia F, Borzacchiello A, Ambrosio L, Rotonda MIL. A novel poloxamers/hyaluronic acid in situ forming hydrogel for drug delivery: rheological, mucoadhesive and in vitro release properties. Eur J Pharm Biopharm. 2008;70(1):199–206.
36. Radivojša M, Grabnar I, Grabnar PA. Thermoreversible in situ gelling poloxamer-based systems with chitosan nanocomplexes for prolonged subcutaneous delivery of heparin: design and in vitro evaluation. Eur J Pharm Sci. 2013;50(1):93–101.